



## ORIGINAL ARTICLE

# Abiraterone switches castration-resistant prostate cancer dependency from adrenal androgens towards androgen receptor variants and glucocorticoid receptor signalling

J. Matthijs Moll MD<sup>1</sup>  | Johannes Hofland MD, PhD<sup>2,3</sup> | Wilma J. Teubel<sup>1</sup> | Corina M. A. de Ridder<sup>1</sup> | Angela E. Taylor PhD<sup>3</sup> | Ralph Graeser PhD<sup>4</sup> | Wiebke Arlt MD DSc FRCP FMedSci<sup>3</sup> | Guido W. Jenster PhD<sup>1</sup> | Wytse M. van Weerden PhD<sup>1</sup> 

<sup>1</sup>Department of Urology, Erasmus MC, Rotterdam, The Netherlands

<sup>2</sup>Department of Endocrinology, Erasmus MC, Rotterdam, The Netherlands

<sup>3</sup>Centre for Endocrinology, Diabetes and Metabolism (CEDAM), School of Clinical and Experimental Medicine, University of Birmingham, Birmingham, UK

<sup>4</sup>Department of Translational Medicine and Clinical Pharmacology, Boehringer Ingelheim Pharmaceuticals, Inc., Ridgefield, Connecticut, USA

## Correspondence

JM Moll, Department of Urology, Erasmus University Medical Center, Postbus 2060, 3000 CB Rotterdam, The Netherlands.  
Email: [j.moll@erasmusmc.nl](mailto:j.moll@erasmusmc.nl)

## Funding information

IMI-PREDECT, Grant/Award Number: Grant agreement n° 115188

## Abstract

**Introduction:** Castration-resistant prostate cancer (CRPC) remains dependent on androgen receptor (AR) signalling, which is largely driven by conversion of adrenal androgen precursors lasting after castration. Abiraterone, an inhibitor of the steroidogenic enzyme CYP17A1, has been demonstrated to reduce adrenal androgen synthesis and prolong CRPC patient survival. To study mechanisms of resistance to castration and abiraterone, we created coculture models using human prostate and adrenal tumours.

**Materials and Methods:** Castration-naïve and CRPC clones of VCaP were incubated with steroid substrates or cocultured with human adrenal cells (H295R) and treated with abiraterone or the antiandrogen enzalutamide. Male mice bearing VCaP xenografts with and without concurrent H295R xenografts were castrated and treated with placebo or abiraterone. Response was assessed by tumour growth and PSA release. Plasma and tumour steroid levels were assessed by LC/MS-MS. Quantitative polymerase chain reaction determined steroidogenic enzyme, nuclear receptor and AR target gene expression.

**Results:** In vitro, adrenal androgens induced castration-naïve and CRPC cell growth, while precursors steroids for de novo synthesis did not. In a coculture system, abiraterone blocked H295R-induced growth of VCaP cells. In vivo, H295R promoted castration-resistant VCaP growth. Abiraterone only inhibited VCaP growth or PSA production in the presence of H295R. Plasma steroid levels demonstrated CYP17A1 inhibition by abiraterone, whilst CRPC tumour tissue steroid levels showed no evidence of de novo intratumoural androgen production. Castration-resistant and abiraterone-resistant VCaP tumours had increased levels of AR, AR variants and

This is an open access article under the terms of the Creative Commons Attribution-NonCommercial License, which permits use, distribution and reproduction in any medium, provided the original work is properly cited and is not used for commercial purposes.

© 2022 The Authors. *The Prostate* published by Wiley Periodicals LLC.

glucocorticoid receptor (GR) resulting in equal AR target gene expression levels compared to noncastrate tumours.

**Conclusions:** In our model, ligand-dependent AR-regulated regrowth of CRPC was predominantly supported via adrenal androgen precursor production while there was no evidence for intratumoural androgen synthesis. Abiraterone-resistant tumours relied on AR overexpression, expression of ligand-independent AR variants and GR signalling.

#### KEYWORDS

abiraterone, adrenal androgens, androgen synthesis, AR variants, castration resistant prostate cancer, CYP17A1 inhibition, glucocorticoid receptor, xenograft

## 1 | INTRODUCTION

Androgen receptor (AR) reactivation is a major driver of castration-resistant prostate cancer (CRPC) and the majority of CRPC tumours remain AR dependent. A substantial proportion of CRPC tumours contain equal amounts of 5 $\alpha$ -dihydrotestosterone (DHT) compared to tumours growing in noncastrate hosts.<sup>1</sup> It has been generally accepted that CRPC tissue can generate its own androgens via conversion of the adrenal precursor steroids dehydroepiandrosterone (DHEA) and androstenedione into DHT, with CRPC tumours abundantly expressing markers for these conversions.<sup>2,3</sup> More controversially, preclinical CRPC models have been reported to possess the potential for de novo androgen synthesis from cholesterol.<sup>4–6</sup>

Advances were made in the hormonal treatment of CRPC by the introduction of the steroid synthesis inhibitor abiraterone [Zytiga<sup>®</sup>]<sup>7,8</sup>—which blocks synthesis of the testosterone precursor DHEA via CYP17A1 inhibition—and the antiandrogen enzalutamide [Xtandi<sup>®</sup>].<sup>9,10</sup>

Multiple mechanisms leading to resistance to second-line hormonal therapies have been described. Resistance to abiraterone and enzalutamide has been linked to increased intratumoural androgen synthesis via the classical<sup>5,11</sup> or the alternative synthesis pathway.<sup>12</sup> Mutations in the ligand-binding domain and overexpression of the AR allowing promiscuous binding of the AR to steroids other than the classical androgens<sup>13</sup> (e.g. progestens or glucocorticoids) have been described for abiraterone<sup>14</sup> and enzalutamide.<sup>15</sup> In addition, AR amplification<sup>15</sup> and expression of ligand-independent AR variants<sup>16,17</sup> have been associated with resistance to abiraterone and enzalutamide. Also, increased glucocorticoid receptor (GR) signalling, taking over part of the transcriptional program of the AR, has been described as a mechanism for primary and secondary resistance to both castration<sup>18</sup> and enzalutamide.<sup>18,19</sup> In patient derived xenografts, GR expression was elevated in tumours with intrinsic and acquired resistance to abiraterone treatment.<sup>20</sup>

However, preclinical research is hampered by significant differences in adrenal steroid biology between humans and rodents. Although we and others found little evidence of CYP17A1-dependent adrenal steroid synthesis in castrate rodents,<sup>21,22</sup> some reports have reported minimal production of androgens in murine adrenal glands after castration.<sup>23,24</sup>

Interestingly, however, in these models CRPC tumours were less affected by treatment with abiraterone than by adrenalectomy,<sup>5,23</sup> questioning an accurate, druggable, representation of human endocrine biology that likely supports CRPC. In this study, we developed in vitro and in vivo coculture models of prostate cancer with human adrenal cells to show that ligand-dependent AR activation in CRPC depends predominantly on androgen precursors secreted by the adrenal gland. Upon abiraterone treatment alternative steroid synthesis pathways, ligand-independent AR (variant) expression and GR expression may subsequently determine drug resistance.

## 2 | MATERIALS AND METHODS

### 2.1 | Cell culture

VCaP and VCaP CRPC subclones (DCC-E, BIC-B, FLU-D<sup>14</sup>) cells were cultured in RPMI 1640 supplemented with 10% fetal calf serum (FCS) or steroid dextran-coated charcoal stripped FCS (DCC) with or without addition of 1  $\mu$ M antiandrogen for CRPC clones and antibiotics. H295R cells—a human adrenocortical tumour cell line which expresses CYP17A1 and subsequently produces high amounts of DHEA and androstenedione<sup>25</sup>—were grown in DMEM/F12, supplemented with 5% FCS and antibiotics. For growth experiments, 5  $\times$  10<sup>3</sup> VCaP cells were plated in 96-well culture plates (Corning) in RPMI supplemented with 10% dextran-coated charcoal stripped FCS (DCC) and antibiotics and left to attach overnight. Cultures were incubated with steroids similar at serum levels found in 60-year-old men and men undergoing ADT<sup>26,27</sup> with 0.1 nM DHT as a positive control based on our experiences in quadruplicate (Table S1). After 10 days, cell numbers were measured by 3-(4,5-dimethylthiazol-2-yl)-2,5-diphenyltetrazolium bromide (MTT)-assay (Sigma) as published in,<sup>28</sup> with each experiment performed in triplicate. For coculture experiments, 5  $\times$  10<sup>4</sup> VCaP cells were plated in 24-well culture plates (Corning) and in parallel, 1  $\times$  10<sup>4</sup> H295R cells were plated in 24 well culture inserts with 0.4  $\mu$ m pores (Corning), both in RPMI supplemented with 10% DCC and antibiotics. After separate overnight attachment, cultures were combined and incubated with indicated

compounds and left to grow for 9 days, after which cell number was assessed by MTT assay for each separate compartment, with each condition in duplicate.

## 2.2 | Animal studies

All animal studies were performed in accordance with local animal welfare legislation and with permission of the local animal experimentation ethics committee. Intact male NMRI<sup>nu/nu</sup> mice were subcutaneously inoculated with  $5 \times 10^6$  VCaP cells in 100  $\mu$ l matrigel (BD Biosciences) with or without concurrent injection of  $5 \times 10^6$  H295R cells in PBS in the contralateral flank (+ADR $\rightarrow$ ORx). Tumour volume (TV) was measured twice a week using callipers and estimated by  $[(\text{height} \times \text{width})^{1.5} \times 0.5236]$ . At VCaP TV  $>150 \text{ mm}^3$ , animals bearing only VCaP tumours were randomly assigned to sham castration (intact), castration with or without concomitant H295R inoculation (ORx + ADR and ORx, respectively) and all +ADR $\rightarrow$ ORx animals were castrated. Orchiectomy was surgically performed under isoflurane anaesthesia. When tumours progressed after castration (defined as a twofold increase in tumour volume after castration), animals were fed daily with 20% HP- $\beta$ -cyclodextrin (Sigma), adjusted to pH 4.0 (vehicle) or vehicle with 10 mg/ml abiraterone acetate (kindly provided by Janssen, Beerse, Belgium) to reach a final dose of 175 mg/kg. At indicated time points, 50  $\mu$ l blood was drawn via mandibular puncture and stored at  $-80^\circ\text{C}$  until further use. When single tumour volume reached  $>1500 \text{ mm}^3$  or combined TV was  $>2500 \text{ mm}^3$ , animals were anaesthetised and blood was drawn via orbital bleeding, after which animals were euthanized. Blood and tumours were snap frozen and stored at  $-80^\circ\text{C}$  until further use, with a part of each tumour stored separately in paraffin.

## 2.3 | PSA response

Blood was collected in heparin tubes and plasma was separated by centrifugation at 1500g for 5 min. PSA was quantified by enzyme-linked immunoassay, using the Elecsys total PSA immunoassay on a Cobas e602 analyzer (Roche Diagnostics). PSA response after castration was calculated as the % increase or decrease vs that of PSA at time of (sham) castration, PSA response after treatment was calculated as the % increase or decrease versus that of PSA at time of treatment initiation.

## 2.4 | Messenger RNA (mRNA) expression analysis

RNA was isolated using RNA-Bee (TEL-TEST, Inc.) from frozen tumour pieces. Reverse transcriptase and quantitative polymerase chain reaction (qPCR) runs were performed as described previously<sup>13</sup> using an ABI Prism 7900 Sequence Detection System under standard conditions. Complementary DNA (cDNA) (20 ng) was amplified in SYBR Green PCR Master Mix (Applied Biosystems) or TaqMan Universal Master Mix (Applied Biosystems). PCR efficiency was verified

by cDNA dilution curves and exceeding 90% for all assays. Primer/probe sets used were AR (forward 5'-CATCAAGGAAGCTCGATCG T-3', reverse 5'-GAACTGATGCAGCTCTCTC-3', probe 5'-ACATCCT GCTCAAGACGCTCCT-3'), PSA (forward 5'-CCCTCAGAAGGTGA CCA-3', reverse 5'-ACCACCTTGGTGTACAGG-3', probe 5'-TATCAC GTCATGGGGCAGTG-3') CYP17A1 (Hs01124136\_m1), CYP11A1 (Hs00167984\_m1), AKR1C3 (Hs00366267\_m1), HSD17B6 (Hs069 55149\_cn). Gene expression was calculated as fold expression over housekeeping genes GAPDH (Hs99999905\_m1) and PBGD (forward 5'-CATGTCTGGTAACGGCAATG-3', reverse 5'-GTACGAGGCTTTC AATGTTG-3') and normalised to the mean expression level from tumours growing in uncastrated placebo treated animals.

## 2.5 | LC/MS-MS quantification of tumour steroid concentration

Steroids were extracted from 200  $\mu$ l of murine plasma or xenograft tissues homogenized in 1 ml milliQ using an Ultra-Turrax T25 (IKA). Following the addition of deuterated steroid controls, liquid-liquid extraction of steroids was performed using tert-methyl-butyl-ether (Sigma-Aldrich). The organic phase was removed after vortexing and evaporated under  $\text{N}_2$  at  $55^\circ\text{C}$ . Samples were reconstituted in 50/50 methanol/water and analysed by liquid chromatography/tandem mass spectrometry (LC-MS/MS) employing a Waters Xevo mass spectrometer with Acquity uPLC system according to conditions previously described.<sup>29,30</sup> Steroids were identified through matching retention times and two mass transitions relative to authentic steroid standards. Quantification was performed relative to a calibration series (range: 0.5–500 ng/ml).

## 2.6 | Immunohistochemistry

Formalin-fixed paraffin embedded tumour pieces were cut, and stained with haematoxylin-eosin. Vital tumour areas were selected for TMA construction with two cores included from each individual tumour. TMA slides were dewaxed, rehydrated, and blocked for endogenous peroxidase activity. Antigen retrieval was performed in sodium citrate buffer (pH 6.0) for 15 min at  $100^\circ\text{C}$ . Antibodies against AR (SP107, 1:200; Spring Bioscience) and GR (611227, 1:500; BD Transduction Laboratories) were diluted in normal antibody diluent (Immunologic) and incubated overnight at  $4^\circ\text{C}$ . Detection of antigens was performed using the DAKO REAL Envision Rabbit/Mouse HRP kit (DAKO) according to standard manufacturer's protocol, after which slides were counter stained with haematoxylin. Images were taken with an Olympus BX41TF microscope equipped with a Olympus Colorview IIIu camera (Olympus). AR expression was quantified by multiplying the fraction of AR positive cells with the staining intensity (0 = no staining, 1 = nuclear, 2 = nuclear + cytoplasmic), GR staining was scored as the percentage of positive cells per field at  $\times 20$  magnification.

## 2.7 | Statistical analysis

Raw data (TV, serum PSA, PSA response) were compared with the appropriate nonparametrical tests. MTT data were analysed by a one-way analysis of variance (ANOVA), followed by a Bonferroni corrected post hoc test to assess significant growth induction by steroids and inhibition by abiraterone and enzalutamide per steroidal condition. qPCR results levels were  $\log_{10}$  transformed to normalize for difference in variance and subsequently compared using a one-way-ANOVA with a Bonferroni posttest. Survival curves were analysed using the Log-rank Test. Endpoint for progression-free survival (PFS) after castration was a fivefold increase in tumour volume (mean + 800 mm<sup>3</sup>), censoring animals started on abiraterone before this endpoint was met. Endpoint for PFS after treatment with abiraterone or placebo was a twofold increase in tumour volume (mean + 450 mm<sup>3</sup>), censoring animals that were euthanized before this endpoint was met. Growth rates were fitted on the %growth for each individual tumour using an exponential growth curve with  $Y = 100$  for  $Y = 100 * e^{(k * x)}$  where Y is the %TV, x is the days postintervention and k is the tumour dependent variable defining the steepness of the curve, correlating to growth rate. All statistical analyses and graphs were made using Graphpad Prism 9.0.

## 3 | RESULTS

### 3.1 | Castration-naïve and CRPC VCaP cell lines are stimulated by physiological levels of adrenal androgens

VCaP cells were incubated with testosterone precursor steroids to test the proliferative effects of physiological steroid levels found in prostate cancer patients (Table S1). CYP17A1 substrates pregnenolone and progesterone failed to induce castration-naïve parental VCaP proliferation (Figure 1A). In contrast, adrenal androgens DHEA and androstenedione induced growth comparable to DHT, which was abolished by direct AR antagonism with 1  $\mu$ M enzalutamide, but not by 0.1  $\mu$ M abiraterone. The abiraterone concentration of 0.1  $\mu$ M was chosen to allow efficient CYP17A1 inhibition, while limiting the direct anti-androgen effect of abiraterone, observed at concentrations >1  $\mu$ M.<sup>13,31</sup> A similar response was observed for the VCaP CRPC clones DCC-E, BIC-B and FLU-D (Figure 1A). Of note, VCaP parental cells treated with vehicle did not divide during the 10-day incubation period, while DCC-E, BIC-B and FLU-D multiplied 3-fold. This growth was unaffected by CYP17A1 inhibition by abiraterone.

### 3.2 | Human adrenal tissue drives castration-resistant growth of VCaP, which can be blocked by CYP17A1 inhibition

To simulate the endocrine system present in men under ADT, human adrenal H295R cells were cocultured with parental and CRPC VCaP cells. H295R stimulated VCaP growth (Figure 1B) similar to DHT.

Addition of 0.1  $\mu$ M abiraterone reduced the H295R-induced proliferation of castration-naïve VCaP and its CRPC clone DCC-E, while not affecting proliferation of VCaP monocultures.

To take this further, we inoculated parental hormone-naïve VCaP cells in intact NMRI nu/nu mice whilst simultaneously inoculating H295R cells contralaterally (Figure 2A). Consistent with the in vitro data, castration of VCaP tumour-bearing mice resulted in a significant reduction in VCaP growth rate (Figure 2B) and serum PSA (Figure 2C). Co-inoculation of H295R cells significantly supported VCaP growth upon castration (+ADR→ORx) compared to VCaP growth in castrate animals without H295R (ORx) (Figure 2B). Despite the supportive effects of H295R on VCaP growth after castration, a clear castration response was still observed in the co-inoculated group, demonstrated by reduced growth rates compared to sham-castrated animals (-Figure 2B) and a reduction in serum PSA 1 week postorchietomy (Figure 2C). Moreover, castration strongly reduced prostate and seminal vesicle weights in castrate animals, with no observed differences were between castrate animals with or without H295R, further demonstrating that H295R cells did not interfere with the systemic state of castration of the host animals (Figure S1).

A PSA rise from nadir was observed in 14/18 castrate animals concomitant with tumour growth, in castrate animals both with and without H295R (Figure 2D). Subsequent Abiraterone treatment at disease progression after castration had a significant impact on VCaP growth and PSA production, but only in castrate animals concomitantly bearing H295R tumours (Figure 2E–G and Figure S2), whilst we were unable to detect a significant difference in tumour growth or PSA production in castrate animals without H295R (ORx). Consistent with these results, in a parallel group of animals co-inoculated with H295R tumours at the time of castration, abiraterone was equally effective in reducing H295R-stimulated VCaP growth and PSA production (Figure S3). Of note, H295R growth was unaffected by castration or abiraterone treatment (Figure S4).

### 3.3 | Endocrine profiles in castration- and abiraterone-resistant VCaP xenografts

Levels of all steroids depicted in Figure 3A were investigated in tumour homogenates and plasma by LC-MS/MS. Testosterone was detectable in homogenates of four out of five VCaP tumours progressive under castration and coinoculated with H295R tumours. Surprisingly, testosterone could still be detected in homogenates of two out of five H295R-unsupported progressive VCaP tumours and three out of five abiraterone-treated sham-castrated VCaP tumours. One out of five castrate animals, but none of the abiraterone-treated intact animals, showed detectable testosterone plasma levels (-Figure 3B). In plasma, DHEA was detectable in four out of five H295R-bearing animals, whilst in tumours, DHEA was found in four out of five placebo-treated H295R tumours and not in any VCaP tumour nor in any abiraterone-treated H295R tumour. Combined, these steroid levels suggest that testosterone found in H295R-supported VCaP tumours could be derived from DHEA secreted by H295R.

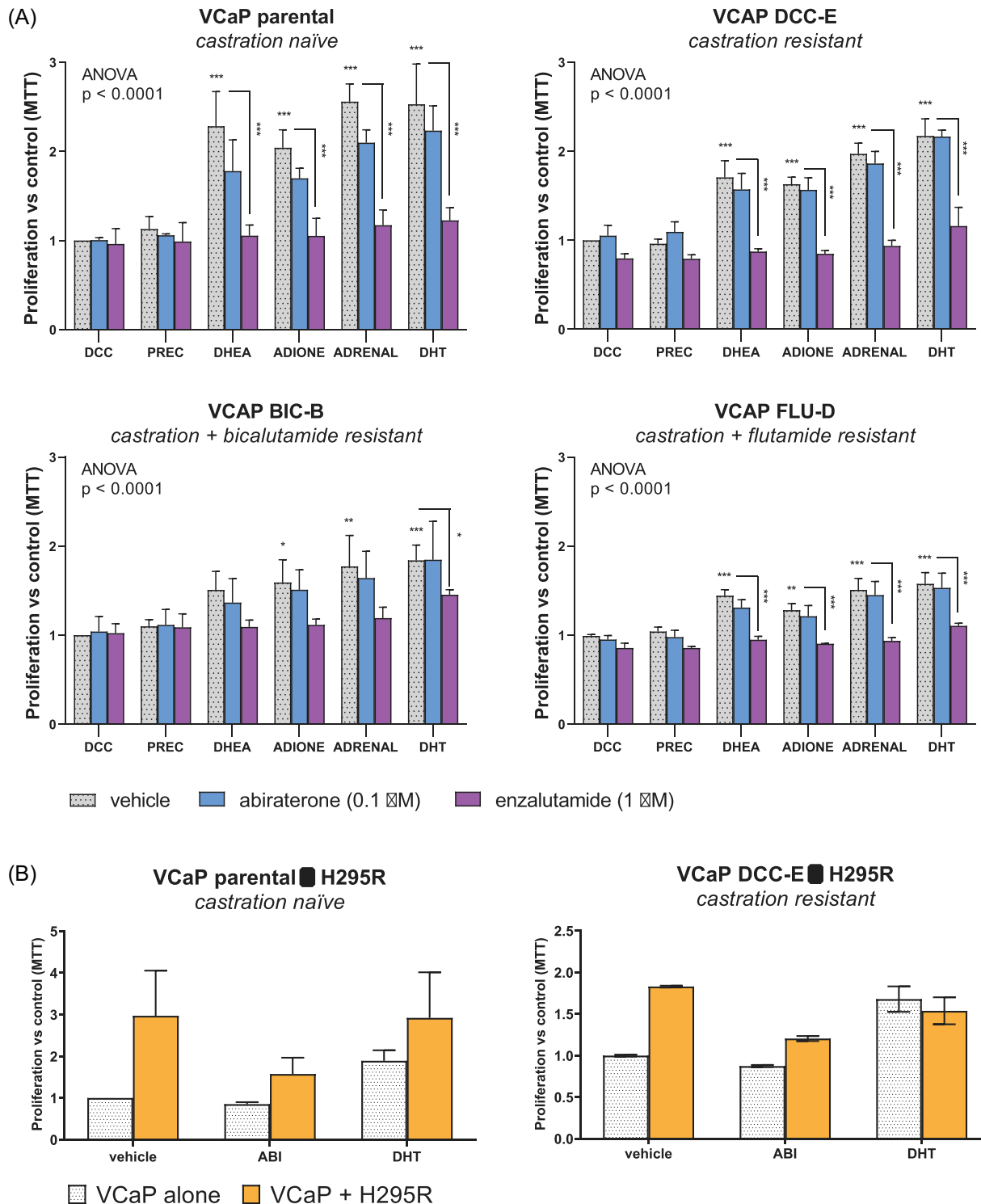


**FIGURE 1** Adrenal steroids and tissue stimulate both castration-naïve and castration-resistant prostate cancer. (A) Growth response of castration-naïve VCaP and its CRPC derivatives (DCC-E, BIC-C, FLU-D) to androgen precursor steroids. Cells were cultured with physiological levels of 1.5 nM pregnenolone and 0.5 nM progesterone combined (PREC), 10 nM DHEA or 2.5 nM androstenedione (ADIONE), the combination of DHEA and ADION (ADRENAL) or 0.1 nM DHT and concomitantly treated with vehicle (DMSO), abiraterone (0.1  $\mu$ M) or enzalutamide (1  $\mu$ M). Bars represent mean fold over control (DCC/DMSO)  $\pm$  SEM. \* $p < 0.05$ , \*\* $p < 0.01$ , \*\*\* $p < 0.001$ . Note: VCaP parental cells did not divide in castrate medium without steroids, whereas VCaP DCC-E, BIC-B and FLU-D divided by an average of threefold. (B) Human adrenal cells induce prostate cancer cell growth under castrate conditions in a two compartment cell culture system. Left: fold growth induction of VCaP parental cells by the human adrenal cell line H295R. Right: fold growth induction of VCaP DCC-E by H295R cells. Abiraterone reduced H295R-induced proliferation, but not basal proliferation in both prostate cancer cell lines. Bars represent mean  $\pm$  SEM. VCaP parental  $n = 3$ , VCaP DCC-E  $n = 1$ . DMSO, dimethyl sulfoxide [Color figure can be viewed at [wileyonlinelibrary.com](http://wileyonlinelibrary.com)]

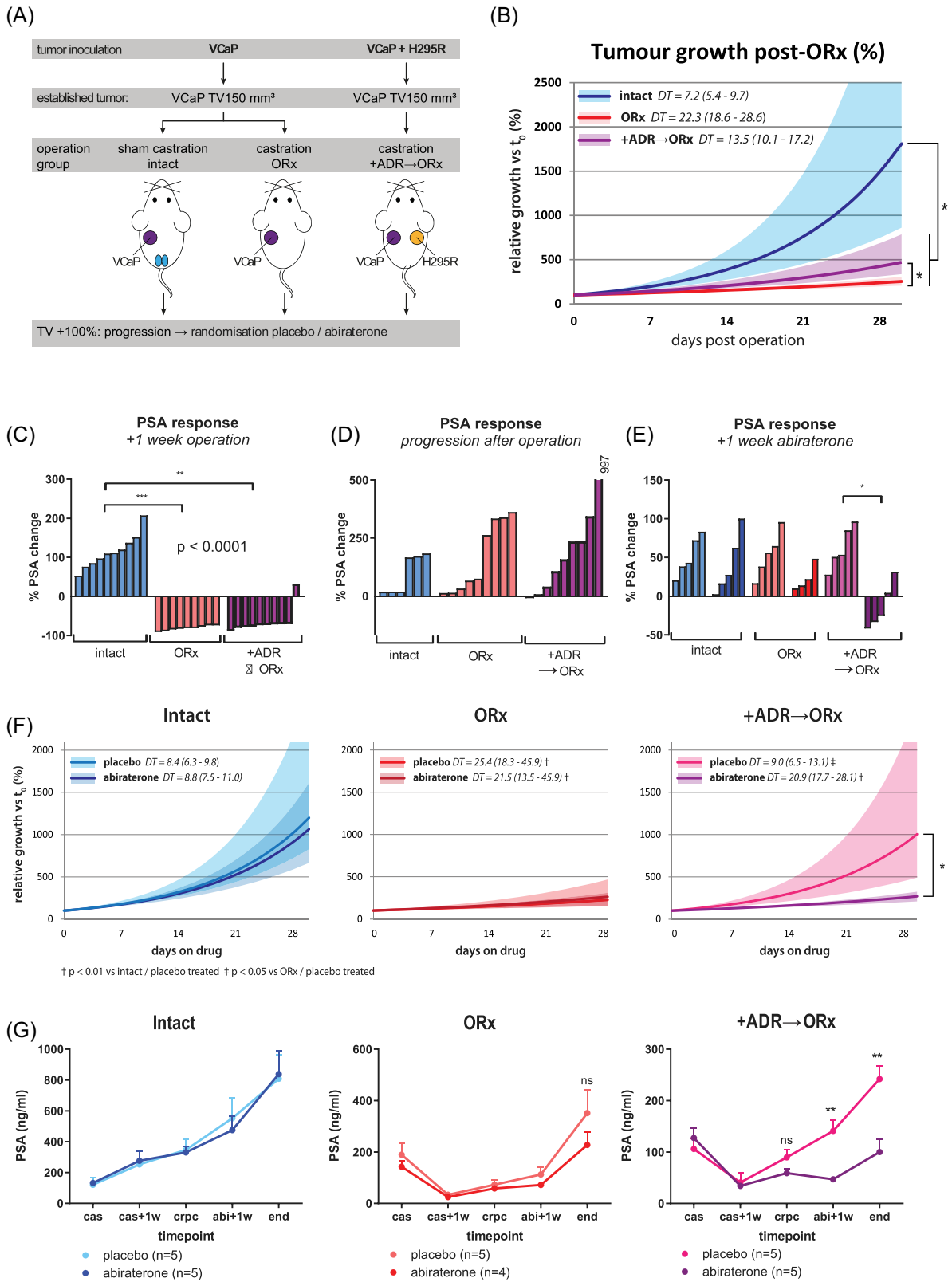


**FIGURE 2** (See caption on next page)

We further analysed mRNA expression for the key steroidogenic enzymes CYP11A1, CYP17A1, AKR1C3, and HSD17B6 (Figure 3A) in VCaP and H295R tumours. As expected, CYP11A1 mRNA was abundantly expressed in H295R while it was below the limit of detection for qPCR ( $ct > 40$ ) in 14 out of 19 VCaP tumours (Figure 3C). CYP17A1 expression was detected in all VCaP tumors at a magnitude (on average: 1100 fold) lower than in H295R, with no alteration by castration or by abiraterone treatment. In contrast, AKR1C3 mRNA was abundantly expressed in VCaP and H295R tumours with slightly higher (fivefold) expression levels in H295R tumours. AKR1C3 expression in VCaP was higher in castrated than in noncastrated hosts, with no additional effect on expression levels by abiraterone treatment. HSD17B6 mRNA was detected in all VCaP tumours at levels above those found in H295R, with no effect of abiraterone treatment on expression levels.

We further evaluated serum levels of intermediates of the alternative androgen synthesis pathway. Although these intermediates accumulated upon blocking CYP17A1 with abiraterone (Figure 3D), this did not result in detectable intratumoural DHT levels (Figure 3B) nor did it result in measurable levels of CYP17A1-dependent downstream metabolites of the alternative androgen synthesis pathway (data not shown).

Finally, serum analysis revealed higher corticosterone levels in castrate animals, either with or without H295R tumours, regardless of abiraterone treatment (Figure 3E), suggesting increased glucocorticoid production in mice upon castration. Moreover, in castrate mice, CYP17A1-hydroxylase-dependent 11-deoxycortisol could be detected, which was unaffected by treatment with abiraterone, except in H295R-bearing mice, where 11-deoxycortisol levels were significantly reduced by abiraterone.

### 3.4 | Castration and abiraterone resistance is mediated via expression of ligand-independent AR (variants) and GR signalling

VCaP tumours progressively growing in castrate hosts showed higher mRNA expression levels of full length AR and AR variants (AR-V1 and AR-V7) as compared to VCaP tumours growing in sham-castrated animals,

with no significant differences in expression level between abiraterone- and placebo-treated animals. In placebo-treated H295R-supported VCaP tumours, AR and AR variant expression was significantly higher compared to intact animals, but lower than in castrate hosts without H295R. In this group, abiraterone significantly increased AR and AR-variant expression, similar to levels found in progressive VCaP tumours from castrate animals without H295R (Figure 4A).

PSA mRNA expression was similar for all VCaP tumours irrespective of H295R support and regardless of abiraterone treatment (Figure 4A). Further analysis of AR target genes, such as *FKBP5*, *TMPRSS2*, *TIPARP*, and *NDRG1*, revealed no statistically significant differences between groups or treatments (Figure 4B), pointing towards restored AR signalling, despite limited detection of intratumoural testosterone and androgen synthesis intermediates in abiraterone-treated tumours. Moreover, expression of the AR target genes *TMPRSS2*, *PSA* and *FKBP5* was correlated with increased expression of full length AR and AKR1C3, but not with increased expression of CYP17A1 (Figure S5).

In parallel with AR, GR expression was elevated in progressive H295R-unsupported VCaP tumours compared to tumours grown in sham-castrated animals irrespective of abiraterone treatment. In H295R-supported VCaP tumours, abiraterone treatment increased GR expression (Figure 4C). Similarly, mRNA for the GR-regulated gene *SGK1* could be detected in all VCaP tumours and was elevated in all castration-resistant and abiraterone-treated H295R-supported tumours, whilst remaining unaltered in the intact arm. Upregulation of GR was significantly correlated with the expression of *SGK1* (Figure 4C). Subgroup analysis indicated that in VCaP tumours with increased expression of GR, *SGK1* was only upregulated in castration-resistant tumours grown without H295R (open and closed red dots) and in abiraterone-treated tumours grown with H295R (purple filled dots) (Figure 4C).

Expression of AR and GR was further validated by immunohistochemistry. In noncastrate animals, AR staining in VCaP tumours was only nuclear. In castrated animals, both with and without H295R tumours, AR staining was intense and also cytoplasmic, indicating these tumours were growing in an androgen-deprived environment (Figure 4D). Immunohistochemistry further

**FIGURE 2** In vivo prostate tumour growth is stimulated by the presence of a human adrenal xenograft, which can be reduced by CYP17A1 inhibition. (A) Flowchart of the in vivo experiment: VCaP tumours were inoculated with or without H295R tumours on the contralateral side. At progression after sham castration or castration, animals were randomised to receive daily oral gavage of abiraterone or placebo. (B) Mean relative growth  $\pm 95\%$  CI of placebo treated animals from castration to humane endpoint. Growth rates were significantly lower in castrate animals compared to intact animals (pooled students  $t$ -test  $p = 0.0012$ , trend  $p = 0.0012$ ). Growth rates were significantly higher in animals co-inoculated with H295R cells (+ADR $\rightarrow$ ORx) compared to animals without (ORx) (students  $t$ -test  $p = 0.04$ ). DT = tumour doubling time in days. (C) Waterfall plot of PSA response after operation, defined as % PSA change 1 week after sham castration or castration relative to serum PSA at time of operation. Each bar represents an individual animal. Kruskal–Wallis  $p < 0.0001$ . (D) Waterfall plot of PSA response at progression after operation, defined as % PSA change at progression after sham castration or castration relative to PSA nadir after operation. Each bar represents an individual animal. Kruskal–Wallis  $p = 0.81$ . (E) Waterfall plot of PSA response after abiraterone, defined as % PSA change after 1 week of abiraterone treatment relative to PSA at start of treatment. Each bar represents an individual animal. (F) Mean relative growth  $\pm 95\%$  CI of placebo and abiraterone treated animals from start of treatment to humane endpoint, stratified by hormonal arm (intact, ORx, +ADR $\rightarrow$ ORx). Growth rates were only significantly different in the +ADR $\rightarrow$ ORx arm (students  $t$ -test  $p = 0.02$ ) \* $p < 0.05$ . DT = tumour doubling time in days. (G) PSA levels (mean + SEM) per treatment group, stratified by hormonal arm (intact, ORx, +ADR $\rightarrow$ ORx). Mann–Whitney test, \* $p < 0.05$  \*\* $p < 0.01$ . CI, confidence interval [Color figure can be viewed at [wileyonlinelibrary.com](http://wileyonlinelibrary.com)]

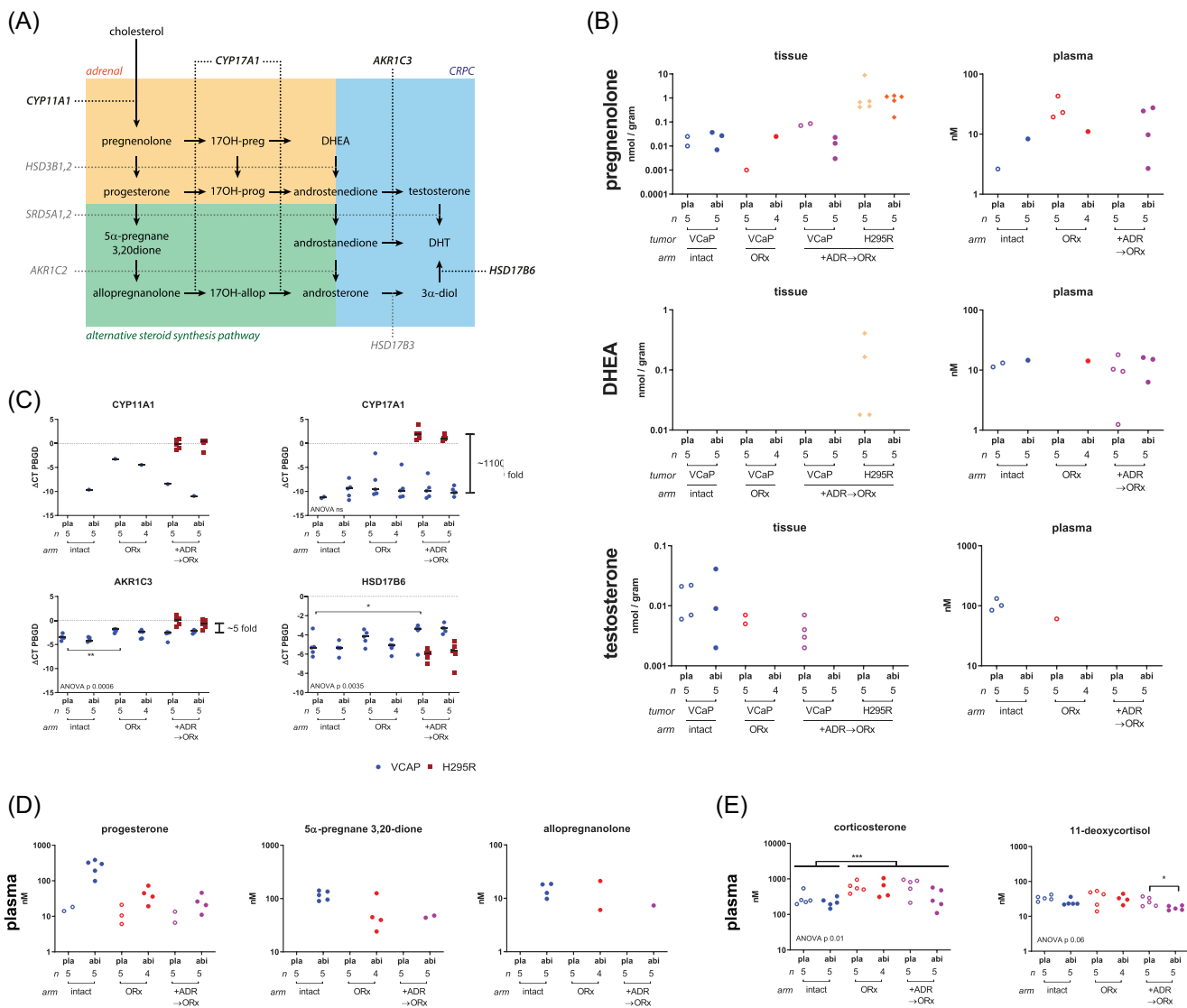


**FIGURE 3** Endocrine profiles of castration- and abiraterone-resistant tumours and hosts. (A) Overview of the classical and alternative steroid synthesis pathway from cholesterol to DHT. (B) Classical testosterone synthesis intermediates. Left: intratumoural levels of the CYP17A1 substrate pregnenolone, the CYP17A1 metabolites DHEA and the androgen testosterone in VCaP tumours and corresponding levels in corresponding H295R tumours for +ADR $\rightarrow$ ORx. Right: corresponding plasma levels of indicated steroids. (C) Steroidogenic enzymes expression. mRNA expression of CYP11A1, CYP17A1, AKR1C3, and HSD17B6 relative to the housekeeping gene PBGD in VCaP and corresponding H295R tumours. Differences between VCaP and H295R were calculated by  $2^{\Delta\Delta CT}$ . (D) Serum levels of intermediates of the alternative steroid synthesis pathway. Steroids could not be detected in tumour homogenates (data not shown). (E) Plasma levels of the main rodent glucocorticoid corticosterone and the CYP17A1-dependent 11-deoxycortisol in castrate male mice at humane endpoint. Dots indicate each measurable datapoint. Unmeasurable samples (ct-value >40 for qPCR or steroid below LOD) not shown in this graph. qPCR, quantitative polymerase chain reaction [Color figure can be viewed at [wileyonlinelibrary.com](http://wileyonlinelibrary.com)]

revealed that in progressive VCaP tumours under castrate conditions, GR localised to the nucleus, whereas GR protein was absent in VCaP tumours grown in sham-castrated hosts (Figure 4E).

## 4 | DISCUSSION

We developed a humanised murine model for CRPC to define the role of adrenal stimuli on progressive prostate cancer in castrated hosts. Physiological levels of adrenal steroids stimulated hormone-

naïve and CRPC growth of VCaP cells, with no such effects induced by substrates of de novo steroid synthesis. The addition of human adrenal (H295R) cells to VCaP cultures and to VCaP-bearing mice stimulated VCaP growth upon androgen depletion. These stimulatory effects could be abolished by treatment with the CYP17A1 inhibitor abiraterone, while abiraterone could not reduce VCaP growth in the absence of human adrenal tissue. These observations together seem to suggest that VCaP tumours were not relying on CYP17A1-dependent, intratumoral de novo steroid synthesis for steroid-dependent AR-stimulus, but that an alternative means to stimulate



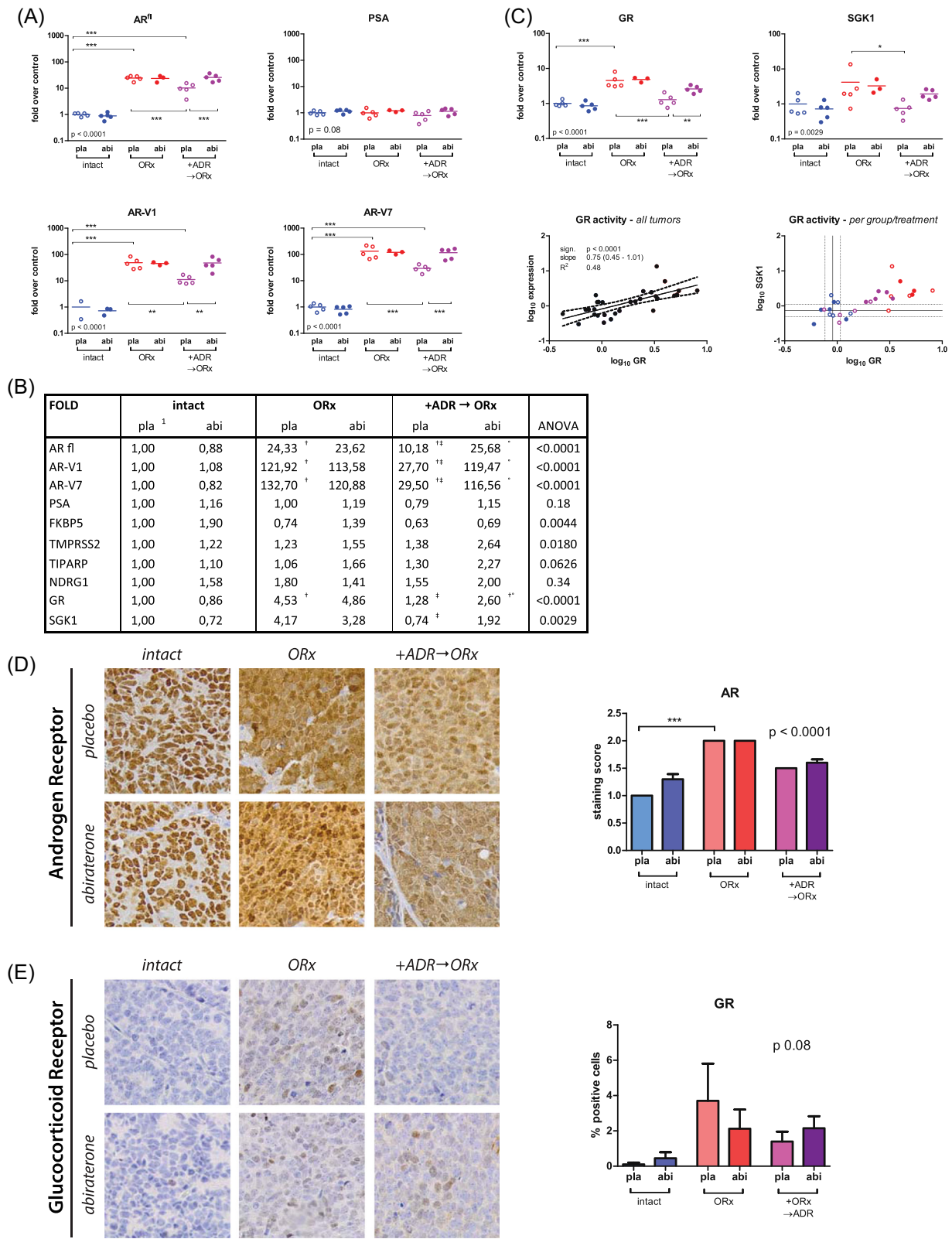


FIGURE 4 (See caption on next page)

growth in the absence of androgens or androgen precursors existed. Steroid profiles in serum and tumour tissues confirmed that indeed both CYP17A1 substrate and CYP17A1 product were hardly detectable in VCaP tumours, whilst being abundant in plasma of tumour bearing mice and H295R tumours. Finally, AR variants and GR signalling were enhanced under abiraterone treatment, suggesting that prostate cancer switches from adrenal androgen dependency to androgen independent steroid receptors.

The supposed lack of adrenal CYP17A1 expression in rodents<sup>32</sup> suggests lack of an androgen-pool in preclinical models that has proven to be highly relevant for prostate cancer progression in patients. To our surprise, we detected low testosterone serum levels in some, but not all castrate mice not engrafted with H295R. Also, CYP17A1-dependent 11-deoxycortisol was detected in all animals together with accumulating serum levels of CYP17A1 substrate progesterone in castrate mice treated with abiraterone. These data indicate that some 17-hydroxylase or 17,20 lyase activity must remain in castrate murine hosts, albeit without concomitant effects on castration-resistant VCaP tumour growth in our study. Potential sources of these steroids may be a partial switch of the adrenal gland to a testicular phenotype upon orchietomy as reported in C57BL6-mice<sup>24</sup> or the reported castration-induced development of adrenal tumours expressing gonadal markers in CE/J-mice.<sup>33</sup> Recently, adrenal expression of CYP17A1 and detection of CYP17A1-dependent metabolites was demonstrated in CB-17 SCID mice.<sup>23</sup> In our study, abiraterone did not affect castration-resistant VCaP growth in the absence of H295R, suggesting no relevant CYP17A1 dependent androgen synthesis in castrate NMRI mice.

In noncastrated hosts, abiraterone did not reduce plasma PSA levels or prostate or seminal vesicle size. These results may be explained by an excess of CYP17A1 in noncastrated animals, rendering abiraterone ineffective. An alternate explanation may be the reported reduced efficacy of abiraterone to inhibit murine CYP17A1 with abiraterone and abiraterone-acetate having an approx. 10-fold higher IC<sub>50</sub> in vitro for rodent CYP17A1 compared to human CYP17A1.<sup>34</sup> This is supported by our observation that abiraterone reduced

11-deoxycortisol levels only in animals co-grafted with (human) H295R. Clearly, these interspecies differences in drug efficacy, alongside the aforementioned interstrain differences in enzyme expression, should be taken into account in further preclinical evaluation of novel steroid synthesis inhibitors and/or modelling of CRPC. We, therefore, believe that the addition of human adrenal tissue creates a mouse model that more accurately recapitulates the endocrine environment found in men.

Still, VCaP tumours progressed in castrate hosts that were not supported by H295R with concomitant AR reactivation in the absence of testosterone or DHT. This may be explained by AR binding to other steroids, like (high levels of) progesterone.<sup>13,14</sup> Indeed, we found that treatment with abiraterone significantly increased plasma levels of progesterone, permitting promiscuous binding of over-expressed AR in abiraterone-treated tumours.

The alternative steroid synthesis pathway has also been proposed as a resistance mechanism for CRPC to treatment with steroids synthesis inhibitors. In this study abiraterone increased plasma levels of alternative steroid intermediates progesterone, 5 $\alpha$ -pregnan-3,20-dione and allopregnanolone, similarly to earlier reports.<sup>12</sup> However, no CYP17A1-dependent downstream metabolites could be detected in plasma or in VCaP tumours, questioning whether the alternative pathway to DHT is active in the presence of abiraterone.

AR variants may also explain persisting AR pathway activity in the absence of ligand. In our study, VCaP tumours progressive after castration expressed higher levels of AR variants compared to tumours grown in a noncastrate hosts. Interestingly, in VCaP tumours growing in castrate hosts expression of variants and full length AR was linearly correlated (Figure S6), questioning the existence of a preferential spliceosome of AR variants in CRPC as has been suggested.<sup>35</sup>

The rise in serum glucocorticoids in castrate animals corroborates previous reports that AR signalling potentiates the negative feedback by glucocorticoids on the hypothalamic-pituitary-adrenal (HPA) axis.<sup>36</sup> How this HPA axis stimulation may affect CRPC growth remains to be explored, but increased levels of GR and GR signalling

**FIGURE 4** Upregulation of AR, AR variants, GR and target genes in CRPC and abiraterone resistant tumours. (A) Increased expression of full length AR and AR variants. Clockwise from top, left: VCaP tissue mRNA expression of full length Androgen Receptor (AR<sup>fl</sup>), the AR target gene PSA and the ligand independent AR variants 1 and 7. (B) Summary table of mean fold expression changes in mRNA expression levels for AR and AR variants, the AR regulated genes *PSA*, *FKBP5*, *TMPRSS2*, *TIPARP*, *NDRG1*, the glucocorticoid receptor and *SGK1* relative to control (intact/placebo). †Significant difference versus intact/placebo treated tumours; ‡significant difference versus ORx/placebo treated tumours; °significant difference between abiraterone versus placebo treated tumours within arm. <sup>1</sup>Reference expression level. (C) Increased GR signalling in CRPC and abiraterone resistant tumours. Top: Tissue RNA expression of Glucocorticoid Receptor (GR) and the GR target gene serum/glucocorticoid regulated kinase 1 (SGK1). Bottom, left: expression of GR and SGK1 sorted per treatment arm. Dotted lines indicate the 95% CI of the mean expression of GR and SGK1 in the intact group. Although GR expression is also upregulated in the co-inoculated arms, SGK1 expression is only increased in the presence of abiraterone. Bottom, right: correlation of GR and SGK1 expression. (D) Androgen Receptor protein expression. Left: representative images of VCaP tumours (magnification ×20). Right: quantification of AR staining score as defined by multiplying the fraction of AR positive cells with staining intensity (0 = no staining, 1 = nuclear, 2 = nuclear + cytoplasmic) scored at magnification ×20. Statistical test using one-way ANOVA with Bonferroni posttest: \*\*\**p* < 0.001. (E) Glucocorticoid Receptor protein expression. Left: representative images of VCaP tumours, (magnification ×20). Right: quantification of GR positive cells as percentage of positive cells per field at ×20 magnification. Statistical test using one-way ANOVA. ANOVA, analysis of variance; CRPC, castration-resistant prostate cancer; GR, glucocorticoid receptor; mRNA, messenger RNA [Color figure can be viewed at [wileyonlinelibrary.com](http://wileyonlinelibrary.com)]

have been reported in CRPC,<sup>18</sup> enzalutamide-resistant disease<sup>19</sup> and in abiraterone-resistant disease.<sup>20,23</sup> This is of particular interest, as a clinical phase 2 abiraterone trial demonstrated superiority of concomitant administration of dexamethasone vs prednisone at a threefold lower equivalent daily glucocorticoid dose.<sup>37</sup> On the contrary, in a post hoc analysis of the COU-AA-301 trial, corticosteroid use at baseline was associated with a worse overall prognosis, but not with less response to abiraterone.<sup>38</sup> Clearly, further studies are warranted to investigate if targeting the GR in the setting of CRPC and abiraterone resistant prostate cancer may impair disease progression.

## 5 | CONCLUSIONS

We have established a humanised murine model for CRPC that mimics the endocrine environment in prostate cancer patients under ADT. We show that human adrenal tissue stimulates prostate cancer growth under castrate conditions. This model is highly responsive to treatment with the CYP17A1 inhibitor abiraterone, whilst tumours growing in absence of adrenal tissue are not. Resistant tumours show high levels of AR, AR variants, but also increased GR signalling, marking these as potential targets for treating abiraterone-resistant disease.

### ACKNOWLEDGEMENTS

We thank A.H. Boer, D.C. Stuurman and S.A.H. Hoeben (Erasmus Medical Centre, Rotterdam, The Netherlands) for their assistance with the animal experiments. We would like to thank S. Blom and K. Valimaki (FIMM, Helsinki, Finland) for their technical support in constructing the tissue micro-array. The research leading to these results has received support from the Innovative Medicines Initiative Joint Undertaking under grant agreement No. 115188, resources of which are composed of financial contribution from the European Union's Seventh Framework Programme (FP7/2007-2013) and EFPIA companies in kind contribution.

### CONFLICT OF INTERESTS

The authors declare that there are no conflict of interests.

### DATA AVAILABILITY STATEMENT

The data that support the findings of this study are available from the corresponding author upon reasonable request.

### ORCID

J. Matthijs Moll  <http://orcid.org/0000-0003-1520-3911>

Wyske M. van Weerden  <https://orcid.org/0000-0003-0324-4804>

### REFERENCES

- Montgomery RB, Mostaghel EA, Vessella R, et al. Maintenance of intratumoral androgens in metastatic prostate cancer: a mechanism for castration-resistant tumor growth. *Cancer Res.* 2008;68(11):4447-4454.
- Hofland J, van Weerden WM, Dits NF, et al. Evidence of limited contributions for intratumoral steroidogenesis in prostate cancer. *Cancer Res.* 2010;70(3):1256-1264.
- Luu-The V, Belanger A, Labrie F. Androgen biosynthetic pathways in the human prostate. *Best Pract Res Clin Endocrinol Metab.* 2008;22(2):207-221.
- Cai C, Chen S, Ng P, et al. Intratumoral de novo steroid synthesis activates androgen receptor in castration-resistant prostate cancer and is upregulated by treatment with CYP17A1 inhibitors. *Cancer Res.* 2011;71(20):6503-6513.
- Mostaghel EA, Marck BT, Plymate SR, et al. Resistance to CYP17A1 inhibition with abiraterone in castration-resistant prostate cancer: induction of steroidogenesis and androgen receptor splice variants. *Clin Cancer Res.* 2011;17(18):5913-5925.
- Locke JA, Guns ES, Lubik AA, et al. Androgen levels increase by intratumoral de novo steroidogenesis during progression of castration-resistant prostate cancer. *Cancer Res.* 2008;68(15):6407-6415.
- de Bono JS, Logothetis CJ, Molina A, et al. Abiraterone and increased survival in metastatic prostate cancer. *N Engl J Med.* 2011;364(21):1995-2005.
- Rathkopf DE, Smith MR, de Bono JS, et al. Updated interim efficacy analysis and long-term safety of abiraterone acetate in metastatic castration-resistant prostate cancer patients without prior chemotherapy (COU-AA-302). *Eur Urol.* 2014;66:815-825.
- Scher HI, Fizazi K, Saad F, et al. Increased survival with enzalutamide in prostate cancer after chemotherapy. *N Engl J Med.* 2012;367(13):1187-1197.
- Beer TM, Tombal B. Enzalutamide in metastatic prostate cancer before chemotherapy. *N Engl J Med.* 2014;371(18):1755-1756.
- Liu C, Lou W, Zhu Y, et al. Intracrine androgens and AKR1C3 activation confer resistance to enzalutamide in prostate cancer. *Cancer Res.* 2015;75(7):1413-1422.
- Attard G, Reid AH, Auchus RJ, et al. Clinical and biochemical consequences of CYP17A1 inhibition with abiraterone given with and without exogenous glucocorticoids in castrate men with advanced prostate cancer. *J Clin Endocrinol Metab.* 2012;97(2):507-516.
- Moll JM, Kumagai J, van Royen ME, et al. A bypass mechanism of abiraterone-resistant prostate cancer: accumulating CYP17A1 substrates activate androgen receptor signaling. *Prostate.* 2019;79(9):937-948.
- Chen EJ, Sowalsky AG, Gao S, et al. Abiraterone treatment in castration-resistant prostate cancer selects for progesterone responsive mutant androgen receptors. *Clin Cancer Res.* 2015;21(6):1273-1280.
- Azad AA, Volik SV, Wyatt AW, et al. Androgen receptor gene aberrations in circulating cell-free DNA: biomarkers of therapeutic resistance in castration-resistant prostate cancer. *Clin Cancer Res.* 2015;21(10):2315-2324.
- Hu R, Dunn TA, Wei S, et al. Ligand-independent androgen receptor variants derived from splicing of cryptic exons signify hormone-refractory prostate cancer. *Cancer Res.* 2009;69(1):16-22.
- Antonarakis ES, Lu C, Wang H, et al. AR-V7 and resistance to enzalutamide and abiraterone in prostate cancer. *N Engl J Med.* 2014;371(11):1028-1038.
- Isikbay M, Otto K, Kregel S, et al. Glucocorticoid receptor activity contributes to resistance to androgen-targeted therapy in prostate cancer. *Hormones & Cancer.* 2014;5(2):72-89.
- Arora VK, Schenkein E, Murali R, et al. Glucocorticoid receptor confers resistance to antiandrogens by bypassing androgen receptor blockade. *Cell.* 2013;155(6):1309-1322.
- Lam HM, McMullin R, Nguyen HM, et al. Characterization of an abiraterone ultrasensitive phenotype in castration-resistant prostate cancer patient-derived xenografts. *Clin Cancer Res.* 2017;23(9):2301-2312.

21. van Weerden WM, Bierings HG, van Steenbrugge GJ, de Jong FH, Schröder FH. Adrenal glands of mouse and rat do not synthesize androgens. *Life Sci.* 1992;50(12):857-861.
22. Michiel Sedelaar JP, Dalrymple SS, Isaacs JT. Of mice and men—warning: intact versus castrated adult male mice as xenograft hosts are equivalent to hypogonadal versus abiraterone treated aging human males, respectively. *Prostate.* 2013;73(12):1316-1325.
23. Mostaghel EA, Zhang A, Hernandez S, et al. Contribution of adrenal glands to intratumor androgens and growth of castration-resistant prostate cancer. *Clin Cancer Res.* 2019;25(1):426-439.
24. Bandiera R, Vidal VP, Motamedi FJ, et al. WT1 maintains adrenal-gonadal primordium identity and marks a population of AGP-like progenitors within the adrenal gland. *Dev Cell.* 2013;27(1):5-18.
25. van der Pas R, Hofland LJ, Hofland J, et al. Fluconazole inhibits human adrenocortical steroidogenesis in vitro. *J Endocrinol.* 2012;215(3):403-412.
26. Bélanger A, Candas B, Dupont A, et al. Changes in serum concentrations of conjugated and unconjugated steroids in 40- to 80-year-old men. *J Clin Endocrinol Metab.* 1994;79(4):1086-1090.
27. Taplin ME, Montgomery B, Logothetis CJ, et al. Intense androgen-deprivation therapy with abiraterone acetate plus leuprolide acetate in patients with localized high-risk prostate cancer: results of a randomized phase II neoadjuvant study. *J Clin Oncol.* 2014;32(33):3705-3715.
28. Kumagai J, Hofland J, Erkens-Schulze S, et al. Intratumoral conversion of adrenal androgen precursors drives androgen receptor-activated cell growth in prostate cancer more potently than de novo steroidogenesis. *Prostate.* 2013;73(15):1636-1650.
29. Haring R, Wallaschofski H, Teumer A, et al. A SULT2A1 genetic variant identified by GWAS as associated with low serum DHEAS does not impact on the actual DHEA/DHEAS ratio. *J Mol Endocrinol.* 2013;50(1):73-77.
30. Jühlen R, Idkowiak J, Taylor AE, et al. Role of ALADIN in human adrenocortical cells for oxidative stress response and steroidogenesis. *PLoS One.* 2015;10(4):e0124582.
31. van Soest RJ, van Royen ME, de Morrée ES, et al. Cross-resistance between taxanes and new hormonal agents abiraterone and enzalutamide may affect drug sequence choices in metastatic castration-resistant prostate cancer. *Eur J Cancer.* 2013;49(18):3821-3830.
32. Payne AH, Hales DB. Overview of steroidogenic enzymes in the pathway from cholesterol to active steroid hormones. *Endocr Rev.* 2004;25(6):947-970.
33. Johnsen IK, Slawik M, Shapiro I, et al. Gonadectomy in mice of the inbred strain CE/J induces proliferation of sub-capsular adrenal cells expressing gonadal marker genes. *J Endocrinol.* 2006;190(1):47-57.
34. Haidar S, Ehmer PB, Barassin S, Batzl-Hartmann C, Hartmann RW. Effects of novel 17 $\alpha$ -hydroxylase/C17, 20-lyase (P450 17, CYP 17) inhibitors on androgen biosynthesis in vitro and in vivo. *J Steroid Biochem Mol Biol.* 2003;84(5):555-562.
35. Nadiminty N, Tummala R, Liu C, Lou W, Evans CP, Gao AC. NF-kappaB2/p52:c-Myc:hnRNPA1 pathway regulates expression of androgen receptor splice variants and enzalutamide sensitivity in prostate cancer. *Mol Cancer Ther.* 2015;14:1884-1895.
36. Chen CV, Brummett JL, Lonstein JS, Jordan CL, Breedlove SM. New knockout model confirms a role for androgen receptors in regulating anxiety-like behaviors and HPA response in mice. *Horm Behav.* 2014;65(3):211-218.
37. Lorente D, Omlin A, Ferraldeschi R, et al. Tumour responses following a steroid switch from prednisone to dexamethasone in castration-resistant prostate cancer patients progressing on abiraterone. *Br J Cancer.* 2014;111(12):2248-2253.
38. Montgomery B, Kheoh T, Molina A, et al. Impact of baseline corticosteroids on survival and steroid androgens in metastatic castration-resistant prostate cancer: exploratory analysis from COU-AA-301. *Eur Urol.* 2015;67(5):866-873.

#### SUPPORTING INFORMATION

Additional supporting information may be found in the online version of the article at the publisher's website.

**How to cite this article:** Moll JM, Hofland J, Teubel W, et al. Abiraterone switches castration-resistant prostate cancer dependency from adrenal androgens towards androgen receptor variants and glucocorticoid receptor signalling. *The Prostate.* 2022;82:505-516. doi:10.1002/pros.24297